

**SPHERICAL NEAR-FIELD ANTENNA MEASUREMENTS  
WITH THE  
SCIENTIFIC-ATLANTA MODEL 2022**

Joseph J. Tavormina  
Scientific-Atlanta, Inc.

Doren W. Hess  
Scientific-Atlanta, Inc.

Abstract

Near-field antenna measurement techniques offer an alternative to conventional far-field antenna measurement techniques. Of the various coordinate systems used for near-field measurements, the spherical coordinate system provides the most natural extension from the conventional far-field characterization of an antenna to a more general characterization for arbitrary range lengths.

This paper describes the Scientific-Atlanta Model 2022, a user-oriented implementation of a spherical near-field antenna measurement system. An example of typical system usage is provided. System capabilities and performance are described. Key concepts required to understand and use the spherical near-field method are discussed.

The advantages and disadvantages of near-field antenna testing in relation to conventional far-field testing are considered. The particular merits of spherical near-field testing as compared to other forms of near-field testing are discussed. Antenna testing situations which provide the most likely candidates for the spherical near-field measurement technique are described.

## Applicability of Near-Field Antenna Testing

The Scientific-Atlanta Model 2022 is an automatic instrumentation/software package designed for the antenna engineer. It is programmed to perform a variety of antenna measurements. A key feature of the Model 2022 is the capability of performing measurements in the near-field of the antenna-under-test. Discussed below are the advantages and disadvantages of near-field antenna testing.

In conventional radiation pattern measurements, a second antenna is used to illuminate the antenna under test with a wavefront that ideally is planar. The measurement consists of recording the received signal at the port of the test antenna as a function of the direction of arrival of the illuminating wavefront. In order for the radiation from the source antenna to approximate a plane wave, the source antenna must lie in the far-field of the antenna under test. For directional test antennas, the separation required to achieve the plane wave condition is often considerable.

Several major drawbacks exist with conventional antenna testing techniques. Since the probe antenna and the test antenna must be separated by a considerable distance, an outdoor antenna range is often required. Consequently, control of the test environment is poor. The antenna test is subject to adverse weather conditions, and pattern measurements are corrupted by ground and other reflections. Also, a sufficiently large tract of land may require a large financial investment.

If the distance requirement permits, conventional testing may be performed in an indoor anechoic chamber.

Indoor testing is generally more convenient than outdoor testing. Stray electromagnetic reflections are greatly reduced indoors by the placement of absorbing material at the ceiling, walls, and floor of the chamber. Control of the environmental temperature and humidity provides for more stable and more reproducible antenna tests. However, the advantages of indoor testing are somewhat costly. The construction cost of an anechoic chamber may be quite high. A large building may be required to house the indoor range; the size of the range is dictated by the distance requirement between the probe antenna and the test antenna. Also, a large quantity of absorption material may be required to line the chamber.

In order to circumvent the distance requirement associated with conventional antenna testing, alternative test methods have evolved. The development of alternative techniques has proceeded along two tracks. The first alternative involves the use of a complex probe configuration. In principle, by utilizing an array of probe antennas in place of a single probe antenna, the spacing between the probe array and the test antenna may be reduced while maintaining a given level of range performance. The compact range technique employs what is effectively a continuous array of sources. A reflective parabolic surface re-radiates energy emitted by a source. Plane wave illumination is thus achieved with a short antenna range.

The compact range test method offers distinct advantages over traditional test methods. Specifically, testing is performed indoors. Thus, all the advantages of indoor testing apply to the compact range technique. Additionally, the chamber required is smaller than that required for a conventional range. Since the required chamber is smaller and less absorbing material is needed, the compact

range is more economical than a conventional indoor range. When comparing the cost of a compact range to an outdoor range, one must consider the required range length and the cost of real estate. The major disadvantage of the compact range technique is the limitation imposed on certain test parameters, especially the size of the test aperture and the range of test frequencies.

Near-field scanning constitutes a second alternative to conventional antenna testing. A small probe antenna is used to sample the near-field radiation pattern of the test antenna. The scanning operation is performed on a geometric surface which completely or partially encloses the volume containing the test antenna. When the near-field radiation pattern has been recorded, a computer algorithm is used to calculate the far-field radiation pattern from the input data.

Near-field scanning can be performed either outdoors or indoors. The distance between the probe antenna and the test antenna is not constrained as in conventional testing. The computer algorithm automatically compensates for range lengths which are too short to provide a far-field radiation pattern. In fact, a primary advantage of near-field scanning is the ability to bring the probe antenna very close to the test antenna, thus reducing the amount of real estate required for an outdoor range or the size of the anechoic chamber required for an indoor range. Another primary advantage of near-field scanning is the high degree of accuracy which can be achieved.

One disadvantage of near-field scanning is the requirement for a computer. A second disadvantage is the time required by the computer to transform the near-field antenna pattern into a far-field pattern. A less obvious drawback is the requirement for data acquisi-

tion on a two-dimensional surface. In general, a one-dimensional cut through a far-field pattern is dependent on many near-field cuts. Thus, two-dimensional data acquisition is necessary even if a single cut of transformed data is all that is desired. Finally, the transformation algorithms used in near-field scanning are limited to antennas which do not exceed a maximum electrical size.

Figure 1 is a comparison of the range configurations which have been discussed. The relative advantages and disadvantages are summarized. Note that with regard to the cost of an antenna range, both the compact range and the near-field range depend on investment in special equipment instead of in land or in buildings.

The major limitations of a conventional outdoor range are the range length and the stray signal level. Relatively poor control of the test environment and of stray signal radiation limits the overall accuracy of a conventional outdoor range. The major limitation of a conventional indoor range is also the range length. This limitation is more severe than on an outdoor range since the facility cost is directly related to the range length. As a result, the overall accuracy of a conventional indoor range is usually compromised by a range length which approaches the minimum allowable. Antenna testing with a compact range is limited by a maximum test aperture, and to a certain range of test frequencies. The overall accuracy of the compact range is related to the surface tolerance of the reflector.

The primary limitation of a near-field range is imposed by the computer algorithm which transforms the near-field pattern to a far-field pattern. The electrical size of the antenna, determined by the size of the test aperture and the wavelength of the test

	<u>Conventional Outdoor</u>	<u>Conventional Indoor</u>	<u>Compact Range</u>	<u>Near-Field Indoor</u>
Land Investment	High	Low	Low	Low
Building Investment	Low	High	Moderate	Moderate
Special Equipment	None	None	Reflector	Computer
Convenience	Poor	Good	Good	Good
Control of Test Environment	Poor	Good	Good	Good
Control of Stray Signals	Poor	Good	Good	Good
Overall Accuracy	Moderate	Good	Good	Excellent
Data Processing Required	No	No	No	Yes
Limitations	Range Length Stray Signals	Range Length	Test Aperture Test Frequency	Electrical Size of Antenna

**Figure 1. Comparison of Range Configurations**

signal, must not exceed the capacity of the transformation software. The overall accuracy of an indoor near-field range is excellent. Performance is not compromised by the finite length of the range, since the computer algorithm automatically compensates for range length. Performance is not dependent upon critical control of machining tolerances, as in the compact range, although care must be taken to assure that the probe remains on the ideal scanning surface. A near-field range utilizes a broad-beamed probe and is electromagnetically simple.

Unlike the other range configurations, far-field test results are not immediately available from a near-field range. Data processing must be performed before the far-field characteristics of the antenna are available. As more experience with near-field methods

is gathered, however, it may become feasible to perform acceptance testing of antennas on the basis of near-field data. If the near-field pattern of the antenna-under-test matches the near-field pattern of a conforming antenna, then the far-field patterns will also match. Acceptance testing on the basis of near-field data would eliminate the time requirement for data transformation, and the requirement to acquire data in two dimensions.

To summarize the application of near-field antenna testing, it is most useful in situations involving physically large antennas of limited electrical size. Such antennas require conventional ranges of excessive length and are too large to test on a compact range. Near-field testing is also applicable when the advantages of indoor testing are desired, but

the cost of a far-field indoor range is prohibitive. Finally, near-field testing is applicable when a high degree of accuracy is required.

### Spherical Near-Field Scanning

Near-field scanning involves the sampling of a radiation distribution on a two-dimensional surface which adjoins the volume containing the test antenna. Three surface geometries are commonly used for near-field scanning. These are a plane, a cylinder, and a sphere. Having chosen the type of scanning surface, the sampling grid can be specified.

Two types of sampling grids for a planar surface are considered here. The first is the cartesian coordinate grid. Figure 2 illustrates near-field scanning on a plane cartesian grid. The sampling surface must extend far enough to intersect the major portion of the energy propagated by antenna. Electromagnetic energy which is outside the coverage of the sampling grid is not accounted for in the calculation of the far-field radiation pattern. The major advantage of plane cartesian scanning is the simplicity of transformation algorithm. The relatively simple mathematics allow for speedy computation of the far-field.

Another coordinate grid which has been considered for scanning a planar surface is the plane hexagonal grid. Figure 3 illustrates near-field scanning in this configuration. The hexagonal grid provides a more efficient sampling arrangement than cartesian grid. The number of samples required to characterize a given radiation pattern is reduced, thus reducing the time required for data acquisition. However, the transformation mathematics for plane hexagonal scanning is more complex than for plane cartesian scanning.

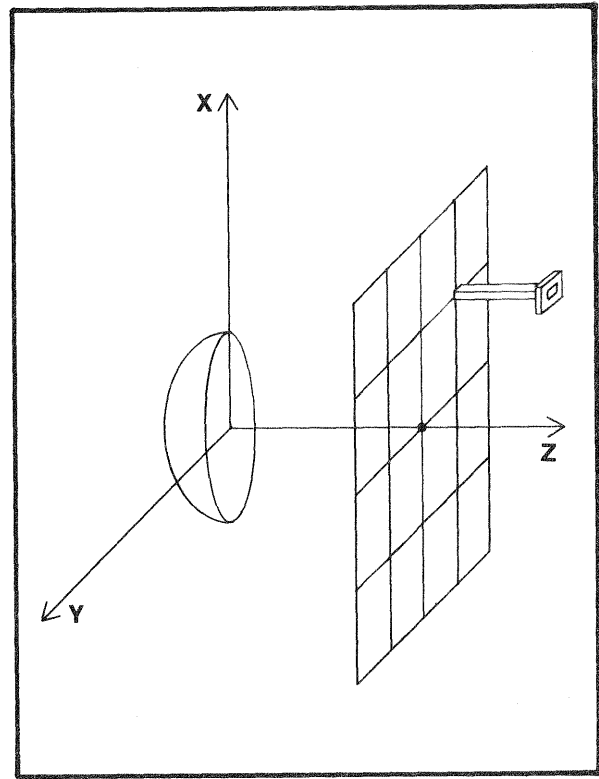


Figure 2. Plane Cartesian Sampling

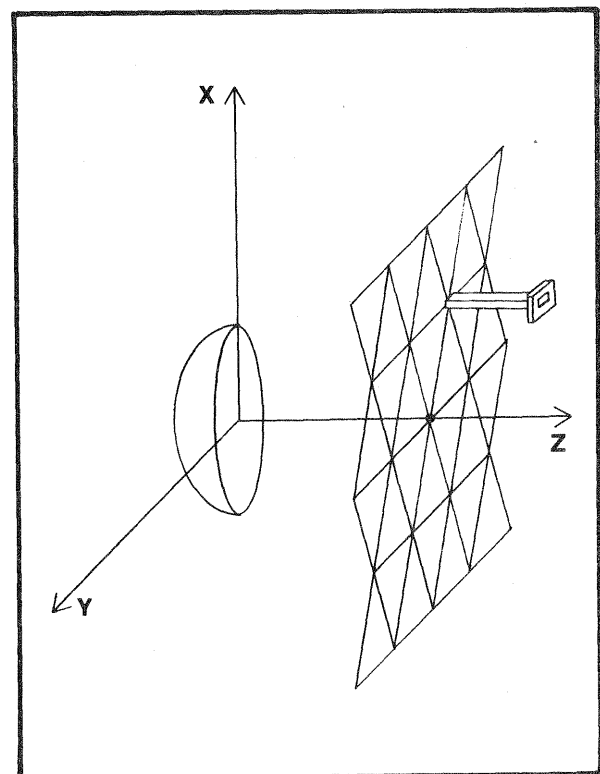


Figure 3. Plane Hexagonal Scanning

The plane hexagonal scanning technique has not been implemented to date. Its consideration has illustrated that the scanning grid is not unique for a given scanning surface. All proper scanning methods will provide the same far-field results, to the extent that the data is acquired accurately and all the energy propagated from the test antenna is accounted for. It is primarily for the sake of convenience in the data acquisition process and in the mathematics of the data transformation that simple sampling grids and regular sampling surfaces are employed.

The usage of a planar sampling surface suffers from several disadvantages. First, the probe positioning problem is difficult. Two perpendicular linear axes are normally employed for positioning the probe in a plane. This positioner configuration is difficult to build and is expensive. Several probe positioners are often required to cover a range of test applications, since the characteristic size and accuracy of the positioner must be scaled to the size of the test antenna and the wavelength of the test signal.

The second potential disadvantage of plane scanning is that the sampling surface cannot enclose the volume of the test antenna. As the sampling surface is enlarged, the degree of closure increases. In the limit, the sampling plane will intercept only half of the directions in which the test antenna might propagate energy. From a practical viewpoint, this might not represent a major concern, since most antennas tested with near-field scanning are highly directional. The planar scanning surface can be arranged to intercept most of the radiated energy. However, the far-field characterization of the antenna can only span a directional range less than a hemisphere.

Cylindrical scanning provides partial solutions to both of the shortcomings of planar scanning. A cylindrical coordinate system with its origin at the test antenna forms the basis for the sampling grid. Figure 4 illustrates cylindrical scanning. Unlike planar scanning, in which the probe is physically moved over the measurement surface, the probe movement in cylindrical scanning is simulated. Physical movement of the probe is limited to the Z-axis. Movements in the  $\theta$ -coordinate are simulated by rotation of the test antenna. Thus, cylindrical scanning requires only one linear axis and one rotary axis. This positioner arrangement is simpler and less expensive than the dual linear axes most often used for planar scanning. The rotary axis does not need to be scaled in proportion to the physical size of the test antenna or the wavelength of the test signal as does the remaining linear axis.

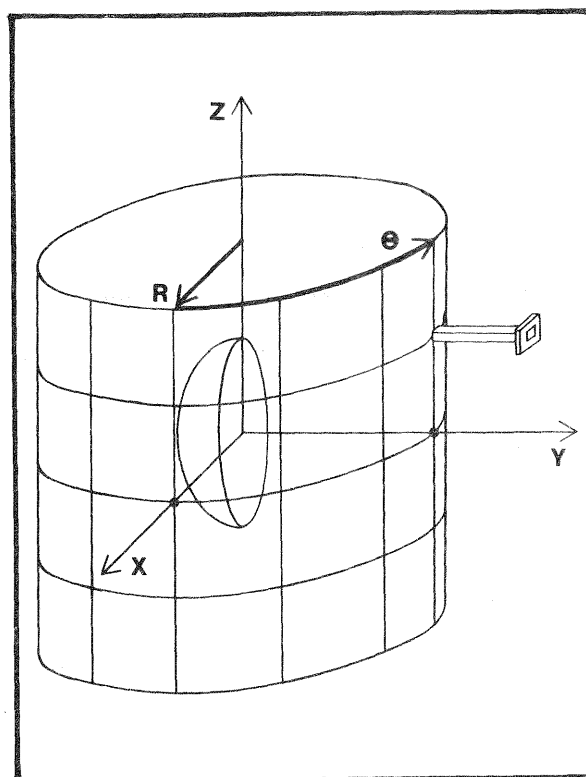


Figure 4. Cylindrical Scanning

Cylindrical scanning does not provide a complete solution to the closure problem since the two end caps of the cylindrical scanning surface are open. Full circular scans are available in one axis however. In the limit, as the Z-span of the cylinder is increased, the scanning surface will intercept all the energy emitted by the test antenna, with the exception of energy propagated along the two poles of the coordinate system.

The primary cost for the benefits of cylindrical scanning is a moderate increase in the complexity of the transformation algorithm. Thus, data processing of cylindrical near-field data takes somewhat longer than the processing of planar cartesian near-field data. This increase in processing time does not represent a major concern, however.

Spherical scanning provides a complete solution to both the scaling problem and the closure problem. In addition, spherical scanning provides other advantages. Figure 5 illustrates spherical scanning. In spherical scanning, the probe is held stationary. Movements in the  $\theta$ -coordinate and in the  $\phi$ -coordinate are simulated by rotation of the test antenna. Spherical scanning does not require any linear motion, and thus completely avoids the scaling problem associated with both planar and cylindrical scanning. The closure problem is also avoided, since the spherical scanning surface completely bounds the volume of the test antenna.

In addition to these advantages, spherical near-field employs positioner configurations which are identical to those used in conventional antenna testing on a far-field range. The major distinction between a spherical near-field range and a conventional far-field range is the degree of separation between the test antenna and the probe antenna. Thus, spherical near-field maximizes the utilization of existing positioner hardware.

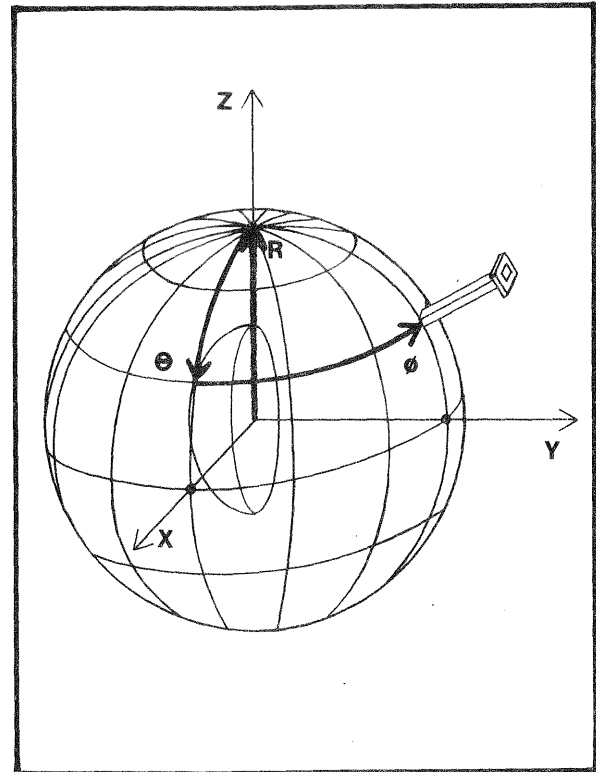


Figure 5. Spherical Scanning

A more subtle advantage of spherical coordinates is the similarity of the near-field and far-field characterizations of the test antenna. In the far-field, the radiation properties of an antenna are expressed as a function of direction. The direction coordinates are the polar and azimuthal angles  $\theta$  and  $\phi$ . Spherical scanning uses these direction coordinates in both the near-field and the far-field of the test antenna, thus providing a natural transition. Near-field data is treated in the same manner as far-field data. For instance, digital pattern plots of near-field data and of far-field data can be generated with the same software. The distinction between the near-field and the far-field is expressed simply as the value of the spherical coordinate  $R$ .

Neither planar nor cylindrical scanning provide this similarity. Planar scanning employs the two linear coordi-

nates X and Y in the near-field. Cylindrical scanning employs the direction coordinate  $\theta$  and the linear coordinate Z in the near-field. In both cases, the transformation algorithms convert the near-field coordinates to spherical direction coordinates in the far-field. Thus, the formats of near-field and far-field data are fundamentally different in planar and cylindrical scanning.

A disadvantage of spherical scanning is a substantial increase in the complexity of the transformation algorithm. The degree of mathematical complexity has been the major impediment to the implementation of spherical near-field. The complexity of the algorithm results in a computation time which is longer than for cylindrical or planar scanning.

Figure 6 is a comparison of the near-field scanning methods discussed above. As can be seen, spherical scanning offers several advantages over planar and cylindrical scanning with only one major disadvantage - that of the transformation algorithm complexity. This does not imply that spherical scanning is the proper choice for every test situation. The choice of scanning geometry may be heavily influenced by the shape of the test antenna. A large flat antenna such as a planar phased array might predicate testing with a planar scanner. Similarly, a tall narrow antenna such as a broadcast antenna may call for testing with cylindrical scanning.

	<u>Plane Cartesian Scanning</u>	<u>Plane Hexagonal Scanning</u>	<u>Cylindrical Scanning</u>	<u>Spherical Scanning</u>
Positioner Configuration	Dual Linear	Dual Linear	Rotary/Linear	Dual Rotary
Scaling Independence	No	No	No	Yes
Complete Closure	No	No	No	Yes
Near/Far-Field Symmetry	No	No	No	Yes
Transformation Complexity	Low	High	Moderate	High

**Figure 6. Comparison of Near-Field Scanning Methods**

## Key Concepts

Having considered the advantages and disadvantages of spherical near-field, an informed judgement can be made as to its applicability in a given test situation. In order to use spherical near-field, however, a basic understanding of certain key concepts must be developed.

### 1. Positioner Configuration

In a spherical near-field range, the test antenna is usually mounted on a dual axis positioner. Both the axes of the test positioner are rotary axes. Figure 7 illustrates several common positioner configurations which may be used for spherical scanning.

In addition to the two axes required to position the test antenna, a third axis is required to control the polarization of the probe antenna. While the two axes which position the test antenna are required to move to a large number of positions, the third axis is normally required to position the probe to only two positions. These two positions correspond to the two orthogonal polarizations of the probe. The two axes which position the test antenna are automatically controlled by the computer during data acquisition. Due to the limited motion of the third axis, a manually controlled positioner is sometimes used.

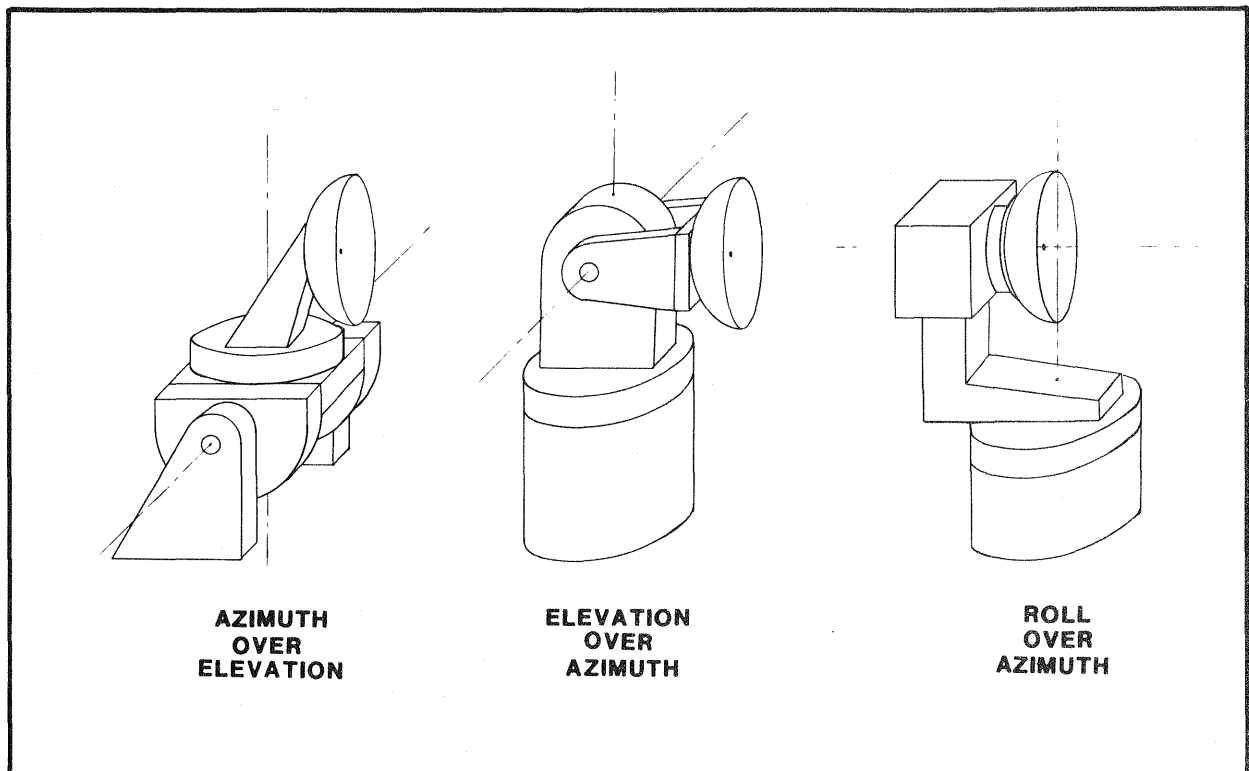


**Figure 7. Common Positioner Configurations**

The three axes required for spherical near-field scanning are labeled theta, phi, and chi. The theta axis is the lower of the two axes used to position the test antenna. The phi axis is the upper of the two axes used to position the test antenna. Chi is the axis used to position the probe antenna. Figure 8 illustrates the axis locations for a near-field range which employs an azimuth-over-elevation test positioner.

Proper alignment of an antenna range places certain constraints on the orientation of the theta, phi, and chi axes. First of all, the theta and phi axes must be orthogonal to each other and must intersect each other. This constraint is satisfied by adjusting the structural components which tie together the two axes

of the test antenna positioner. In addition, the theta and chi axes must be orthogonal to each other and must intersect at the same point that the theta and phi axes intersect. This constraint is satisfied by the proper location and orientation of the probe antenna positioner with respect to the test antenna positioner.

## 2. Positioner Offset Angles

The location of the probe on the spherical scanning surface is given by the spherical coordinates theta, phi, and chi. The spherical coordinates are directly related to the angular readouts of the test positioners. In general, however, an angular offset will exist between the value of a transducer readout and the

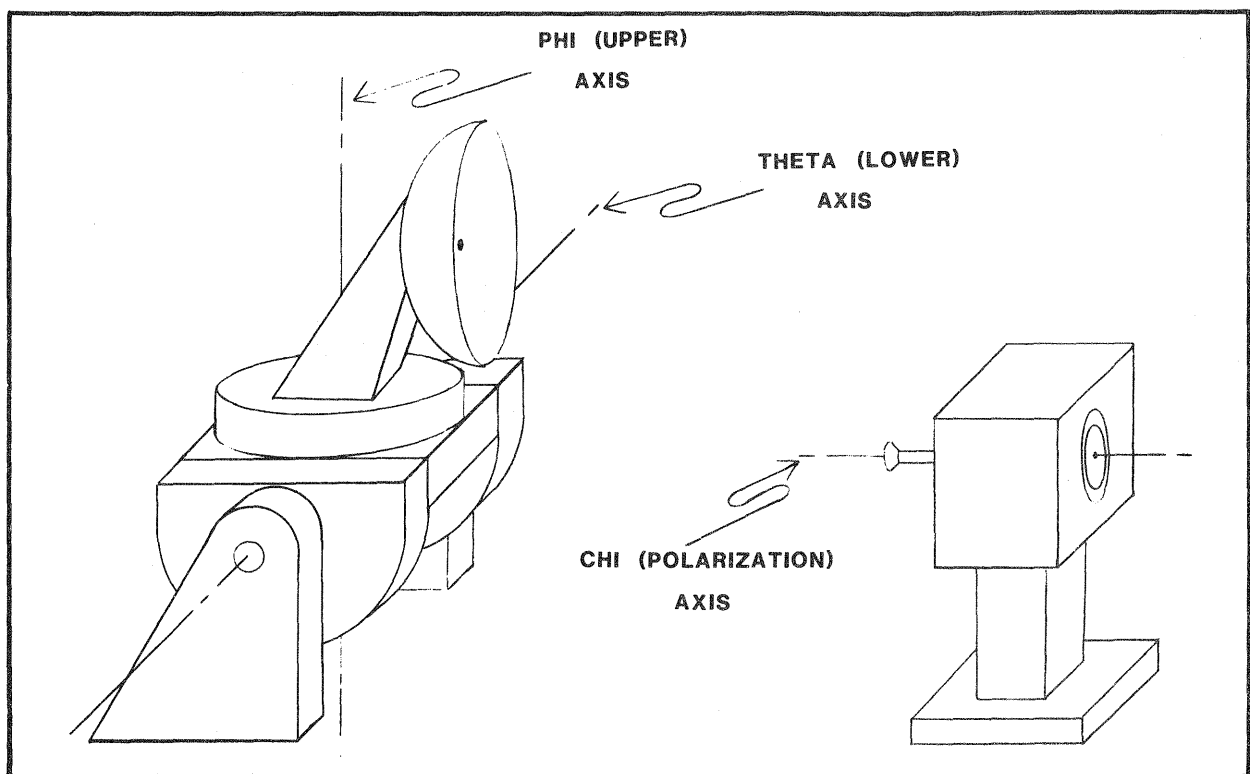


Figure 8. Axis Naming Convention

value of the corresponding mathematical coordinate. In order to transform the acquired data properly, the angular readouts must be calibrated by specifying an offset angle for each of the three axes.

The theta offset angle is the angular readout of the theta axis when it has been rotated such that the phi and chi axes are co-linear. Note that the theta offset angle is independent of the particular mounting of the test antenna. For the azimuth-over-elevation positioner shown in Figure 8, the theta offset angle is the reading on the elevation axis positioner display when the elevation axis has been rotated clockwise so that the azimuth axis and the probe polarization axis overlay.

The phi offset angle is somewhat less critical than the theta offset angle. The phi offset angle describes the center of the antenna pattern insofar as the phi axis is concerned. During data acquisition, the phi axis is scanned so that the position represented by the phi offset angle is midpoint of the scan. For the azimuth-over-elevation positioner shown in Figure 8, the phi offset angle would be the reading on the azimuth axis positioner display for the elevation and azimuth positions shown, presuming that the primary interest is in the test antenna characteristics near the peak of the beam.

The chi offset angle is related to the mounting of the probe antenna on the polarization positioner. The spherical near-field transformation algorithm implemented in the Model 2022 assumes that the probe is linearly polarized. The chi offset angle is the angular readout of the chi axis when the electric field of a transmitting probe is perpendicular to the theta axis. For the range configuration shown in Figure 8, the chi offset angle is the reading on the probe polarization axis

position display when the probe is vertically polarized, since the elevation (theta) axis is horizontal.

### 3. Test Antenna Mounting Configuration

The mounting configuration of the test antenna is described as polar or equatorial. The mounting configuration is normally determined by the orientation of the peak of the radiation pattern in relation to the phi axis. If the peak of the radiation pattern is roughly aligned with the phi axis, the mounting configuration is polar. If the peak of the radiation pattern is roughly perpendicular to the phi axis, the mounting configuration is equatorial.

Both the azimuth-over-elevation configuration and the elevation-over-azimuth configuration shown in Figure 7 illustrate equatorial mounting of the test antenna. In each case, the peak of the radiation pattern is perpendicular to the phi (upper) axis. In the spherical scanning diagram of Figure 5, this corresponds to the main beam of the test antenna intersecting the scanning surface at the equator of the test sphere. Alternatively, the roll-over-azimuth configuration shown in Figure 7 illustrates polar mounting of the test antenna. In this case, the main beam of the test antenna will intersect the scanning surface at the pole of the test sphere.

In infrequent circumstances, the primary interest in the radiation pattern is for a portion other than that portion which adjoins the peak of the beam. In such a case, the mounting configuration of the antenna is determined on the basis of the direction of interest rather than on the basis of the peak direction.

### 4. Minimum Sphere

The minimum sphere represents the smallest scanning surface which

encloses the test antenna. The origin of the scanning surface is the intersection of the theta and phi axes. Thus, the size of the minimum sphere is determined by the positioner configuration and by the manner in which the test antenna is mounted to the positioner as well as by the physical size of the test antenna.

Figure 9 illustrates the minimum sphere for various test configurations. Note that in each case, the center of the sphere is the point at which the theta and phi axes intersect. Note also that certain positioner configurations are more efficient than others in minimizing the size of the minimum sphere.

## 5. Maximum Sampling Interval

The data acquisition process consists of digitally sampling the radiation pattern of the test antenna on the surface of the scanning sphere. The sampled data points are regularly spaced in theta and phi, as shown in Figure 5. In order to speed up the data acquisition process and in order to reduce the data processing time, the sampling interval is made as large as possible. If, however, the sampling interval is made too large, the sampled data set will not provide an adequate description of the continuous radiation pattern. Some of the pattern detail will be lost and the transformed far-field pattern will be in error.

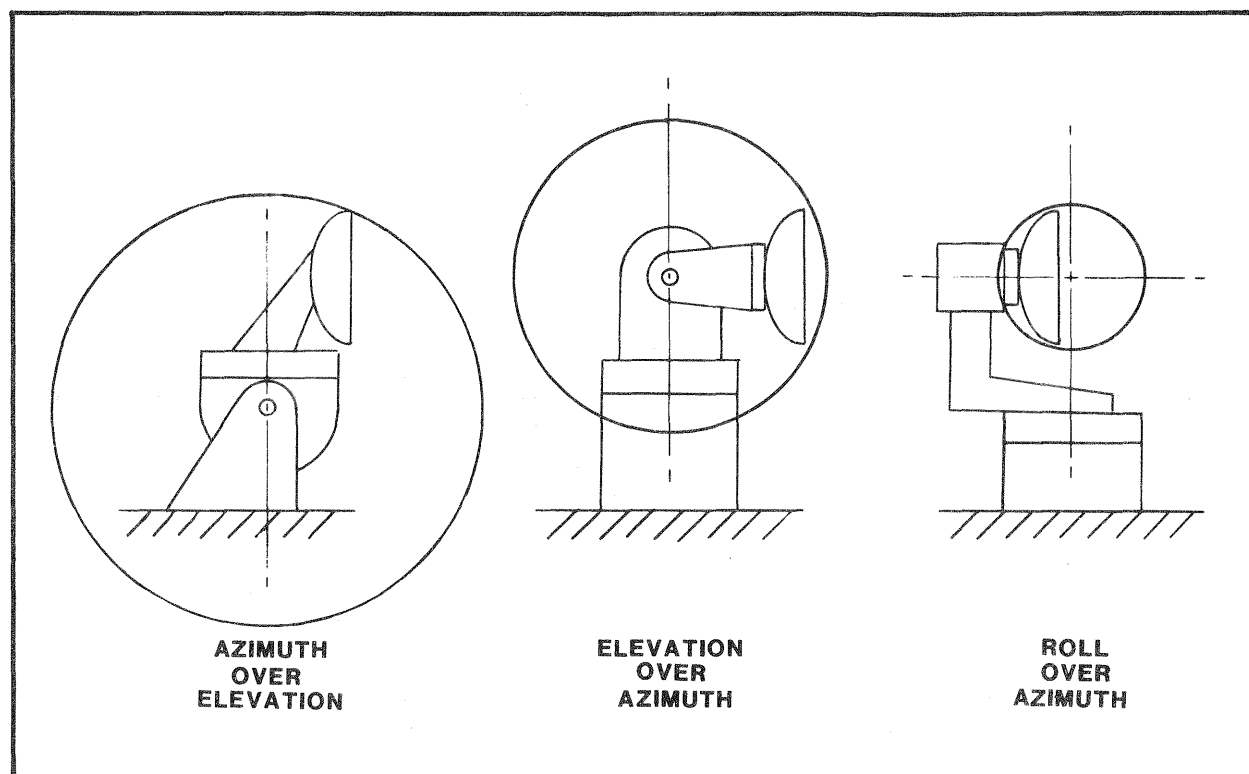


Figure 9. Determination of Minimum Sphere

The theoretical maximum sampling interval which will adequately characterize the radiation pattern is determined by the diameter of the minimum sphere (D) and by the wavelength of the test signal ( $\lambda$ ). These two quantities are used to form the ratio  $D/\lambda$ , which defines the electrical size of the test aperture. As an example, a  $D/\lambda$  ratio of 55 corresponds to a maximum sampling interval of roughly one degree.

Thus, if all the spatial detail of the antenna pattern is to be recorded, the sampling interval for the acquired data must not be greater than the theoretical maximum interval determined from the  $D/\lambda$  ratio. A sampling interval smaller than the theoretical maximum interval may be used, however. While this increases the amount of time required for data acquisition, it does provide the potential to perform pattern filtering and noise rejection. The electrical size of the test aperture determines the maximum rate at which the radiation pattern of the test antenna can change in space. Thus, any spatial frequency components of the acquired data which exceed the maximum spatial frequency are due to noise and may be removed.

### The Model 2022

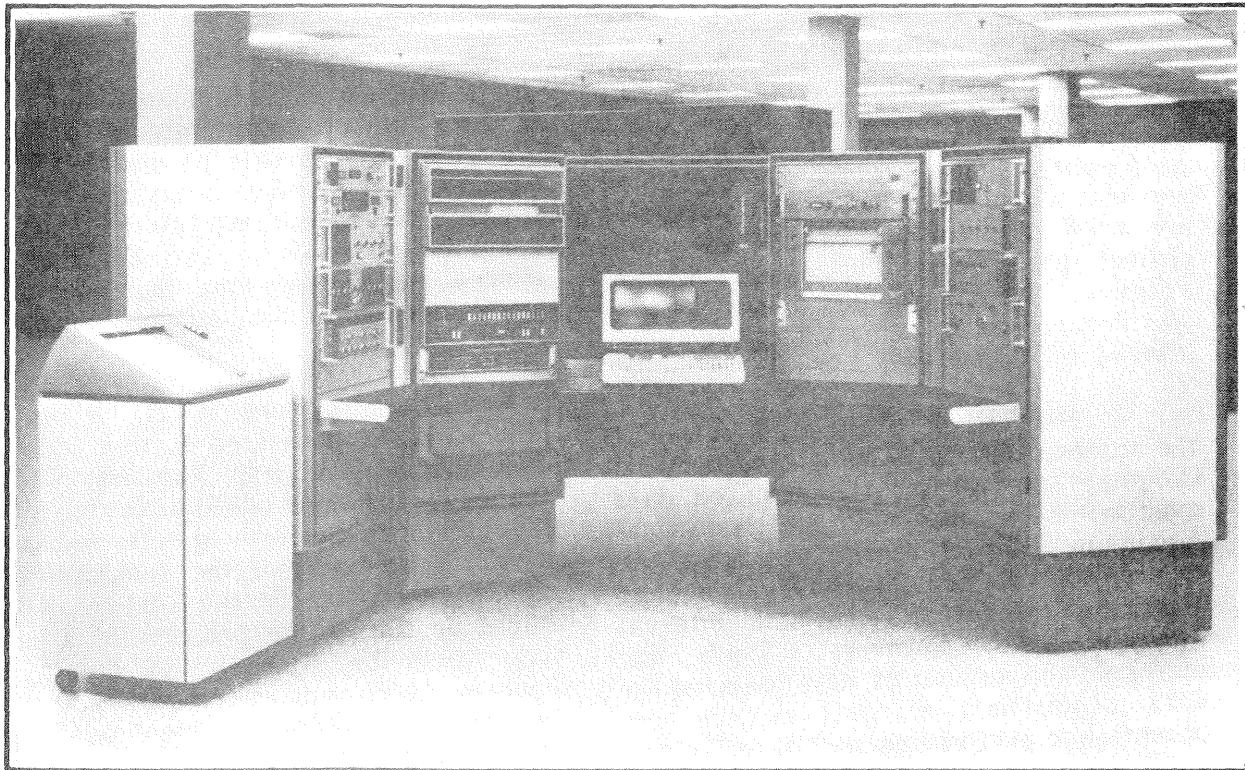
Scientific-Atlanta has implemented spherical near-field as part of its Series 2020 Automatic Antenna Analyzer. The Model 2022 has all the capability of its predecessors, plus the capability to perform spherical near-field data acquisition and data transformation. Attention here is focused on the near-field capability of the Model 2022. Specifications for the other capabilities are available from Scientific-Atlanta.

Figure 10 is a photograph of the Series 2020 Automatic Antenna Analyzer. The Analyzer consists of a signal source subsystem, a receiver subsystem, a positioner controller subsystem, and a computer subsystem. The Analyzer is a general purpose antenna test tool which can be used both manually and automatically.

The software which drives the Model 2022 is organized as four independent operating modes. The first mode is the Keyboard Mode (KBM). In this mode, the user may perform simple operations from the keyboard of the computer console. For instance, the test frequency might be set or the position of a given axis might be altered. In this mode, operator commands at the keyboard simulate the manipulation of front panel controls on the various instruments. This mode is useful for confirming the correct operation of the various instruments which comprise the Model 2022.

A second mode of operation is provided by the Test File Manager (TFM). It is in this mode that automatic data acquisition is programmed and executed. Acquisition parameters are specified by the operator through an interactive dialogue. When the test parameters have been specified, they may be permanently stored on the disc storage unit of the computer as a test file. By issuing the run command, the operator initiates the automatic execution of the specified antenna test. The antenna data acquired during the test is collected on the disc storage unit as a data file.

The Data File Manager (DFM) is a third mode of the Model 2022 software. In this mode the data files created during data acquisition may be accessed. Numerical listings of the collected data may be generated on the system console or



**Figure 10. The 2020 Series Automatic Antenna Analyzer**

on the printer. Data files may be renamed or purged. The DFM Mode is used for maintenance of antenna data.

The fourth operating mode of the Model 2022 software is the Plot File Mode (PFM). As its name implies, PFM permits antenna data to be displayed in a wide variety of graphical formats. Among the output devices which the operator may choose from are the graphic CRT display, the graphic printer, and the Scientific-Atlanta Model 1580 Pattern Recorder.

The spherical near-field capability of the Model 2022 has been implemented as part of the Test File Manager (TFM) Mode. Two new test modules have been added to the existing complement, one for spherical near-field data acquisi-

tion and one for spherical near-field data transformation. Figure 11 illustrates the basic structure of the Model 2022 software.

#### **Spherical Near-Field Data Acquisition**

To acquire near-field antenna data, the operator must invoke the software module that generates a spherical near-field data acquisition test file. This initiates a brief question/answer session with the computer in which the necessary parameters are entered. Upon completion of test file generation, the operator may choose to store the test parameters permanently for later use or to execute

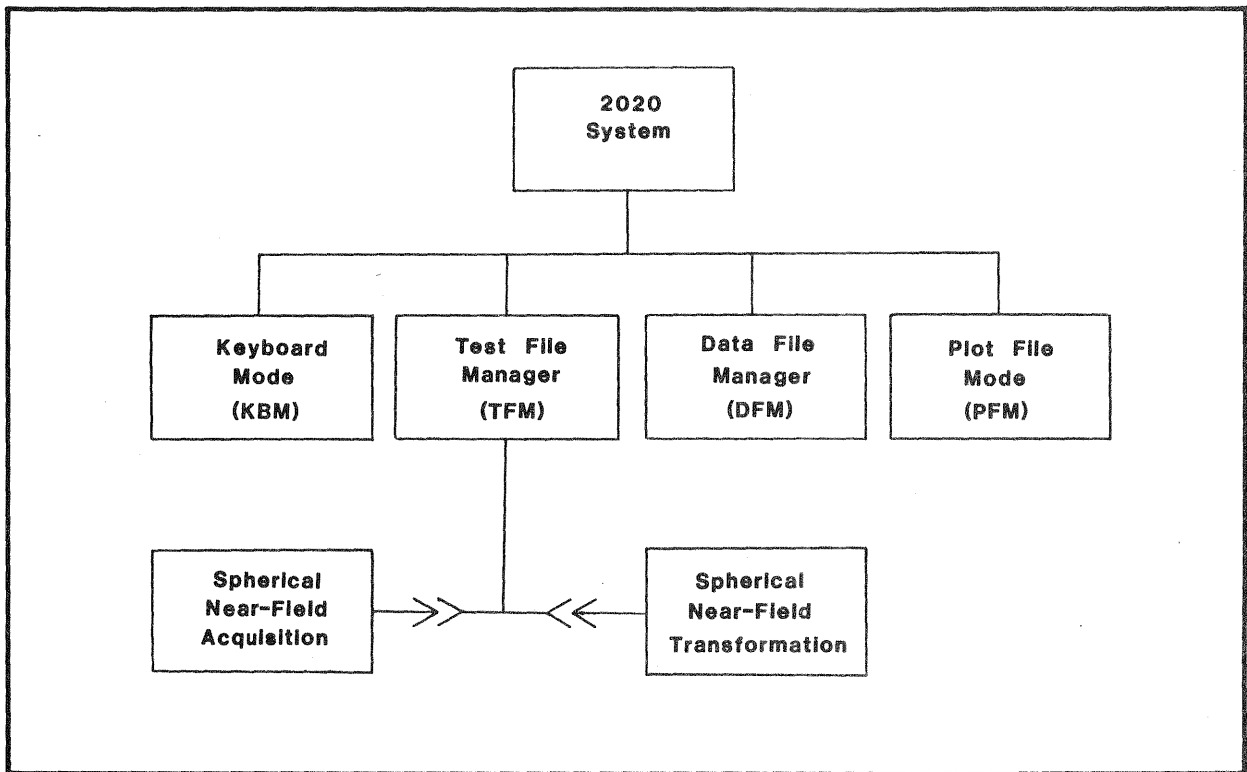


**Figure 11. Model 2022 Software Architecture**

the specified test immediately. Figure 12 is a listing of the test file used to acquire the near-field antenna data shown in subsequent pages.

The acquisition parameters are divided into a number of separate parameter groupings. This helps the operator organize the test parameters and provides access to each parameter group independently during an edit of the test file.

The first group of test parameters specify the configuration of the positioner hardware. The theta, phi, and chi axes are selected from those axes present in the system initialization table. The position readout for each of these axes is calibrated by the entry of the positioner offset angles.

The second group of parameters specify the settings for the auxiliary positioner axes. These are the inactive axes which do not participate in the near-field scanning process. In addition, the initial positions of the theta, phi, and chi axes are specified in this parameter group. If the signal attenuators in the receiver are to be adjusted automatically, the initial position specified should correspond to the orientation of the antenna which produces the maximum received signal.

The third group of test parameters specify the mounting configuration of the test antenna. The radius of the minimum sphere and the acquisition range length are included in this group. Also specified is whether full coverage or partial coverage of the scanning sphere is desired. If partial coverage is specified,

\*SPHERICAL NEAR-FIELD DATA ACQUISITION TEST FILE NUMBER: 65

```
1. TEST POSITIONER CONFIGURATION
*SCAN (PHI) AXIS ID:
  C
*STEP (THETA) AXIS ID:
  A
*PROBE POLARIZATION (CHI) AXIS ID:
  X
*SCAN AXIS OFFSET (PHI ORIGIN) ANGLE (DEGREES):
  22.240
*STEP AXIS OFFSET (THETA ORIGIN) ANGLE (DEGREES):
  .090
*PROBE POLARIZATION AXIS OFFSET (CHI ORIGIN) ANGLE (DEGREES):
  0.000
2. INITIAL POSITION SPECIFICATIONS
*INITIAL AZIMUTH (AXIS A) POSITION:
  90.000
*INITIAL ELEVATION (AXIS B) POSITION:
  -.050
*INITIAL AUT POLARIZATION (AXIS C) POSITION:
  22.240
*INITIAL SOURCE POLARIZATION (AXIS E) POSITION:
  3.000
*INITIAL AUXILIARY 1 (AXIS D) POSITION:
  -40.000
3. TEST ANTENNA CONFIGURATION
*RADIUS OF MINIMUM SPHERE (CENTIMETERS):
  86.000
*CURRENT RANGE LENGTH (CENTIMETERS):
  299.200
*ANTENNA PATTERN COMPLETELY COVERS TEST SPHERE.
4. TEST FREQUENCY SPECIFICATIONS
*ACQUISITION TEST FREQUENCIES (MEGAHERTZ):
  FREQUENCY( 1) - 13000.
5. RECEIVER SET-UP SPECIFICATIONS
*CRYSTAL CURRENT SET AUTOMATICALLY.
*RECEIVER IF MODE:
  DUAL
*ATTENUATOR SETTINGS (DECIBELS):
  FREQUENCY( 1) - 0 (CHANNEL A), 0 (CHANNEL B)
6. ACQUISITION SCAN PARAMETERS
*THEORETICAL MAXIMUM ACQUISITION INCREMENT (DEGREES) = .760
*RECOMMENDED ACQUISITION SCAN INCREMENT (DEGREES) = .750
*RECOMMENDED ACQUISITION SCAN START ANGLE (DEGREES) = -157.760
*RECOMMENDED ACQUISITION SCAN STOP ANGLE (DEGREES) = -158.510
*ACQUISITION SCAN INCREMENT (DEGREES):
  .750
*ACQUISITION SCAN START ANGLE (DEGREES):
  -157.760
*ACQUISITION SCAN STOP ANGLE (DEGREES):
  -158.510
*ACQUISITION SCAN SPEED (PERCENTAGE OF MAXIMUM):
  100
*DATA NOT RECORDED ON SCAN AXIS RETRACE.
7. ACQUISITION STEP PARAMETERS
*THEORETICAL MAXIMUM ACQUISITION INCREMENT (DEGREES) = .760
*RECOMMENDED ACQUISITION STEP INCREMENT (DEGREES) = .750
*RECOMMENDED ACQUISITION STEP START ANGLE (DEGREES) = .090
*RECOMMENDED ACQUISITION STEP STOP ANGLE (DEGREES) = 179.340
*ACQUISITION STEP INCREMENT (DEGREES):
  .750
*ACQUISITION STEP START ANGLE (DEGREES):
  .090
*ACQUISITION STEP STOP ANGLE (DEGREES):
  179.340
8. ACQUISITION PROBE POLARIZATION PARAMETERS
*SINGLE PROBE ORIENTATION.
*PROBE ORIENTATION PARALLEL TO STEP (THETA) AXIS.
9. CRT CONFIRMATION PLOTS
*CONFIRMATION PLOTS MADE.
*END OF TEST FILE LISTING
```

Figure 12. Spherical Near-Field Acquisition Test File

additional information as to the limits of coverage must be entered. Antenna data which is not acquired will be ignored during the calculation of the transformed pattern. When the transformation algorithm requires uncollected antenna data, a null signal is assumed.

The fourth and fifth parameter groups specify the test frequency and the receiver settings, respectively. Up to five test frequencies may be specified for a data acquisition test. In general, when the data acquisition speed is limited by the data transfer rate of the system, no advantage will be gained by multi-frequency operation. If, however, the positioner hardware limits the data acquisition speed, it may be possible to collect data for several frequencies in the same time it takes to collect data for a single frequency.

In the sixth parameter group, the scan ( $\phi$ ) axis sampling parameters are entered. In the seventh group, the step ( $\theta$ ) axis parameters are entered. These specifications consist of the record increments, the start angles, and the stop angles for the  $\theta$  and  $\phi$  axes. The choice of acquisition increments is restricted by data processing considerations. The acquisition increments must divide the sphere into an integral number of sample intervals. The number of intervals must be compatible with the transformation algorithm. The acquisition start and stop angles are also restricted. The scan start and stop parameters must be chosen such that a sample point falls at the scan offset position. The step parameters must be chosen such that a sample point falls at the pole of the spherical scanning surface.

To aid the operator in the selection of appropriate parameters, the computer determines recommended parameter values. On the basis of the minimum sphere specified in the third

parameter group, and the highest test frequency specified in the fourth parameter group, the computer determines the theoretical maximum sample interval. A recommended sample interval somewhat smaller than the theoretical maximum interval is then selected to satisfy the data processing constraint. Next, on the basis of the coverage parameters entered in the third parameter group, the recommended start and stop angles are determined. These recommended values are listed by the computer and serve as the default responses for the queries which follow.

The operator may choose to override the parameter values selected by the computer. In this event, the operator's entry will be checked to insure validity. A valid entry must satisfy all the sampling constraints.

The eighth parameter group specifies whether data is to be acquired for both probe polarizations or for only one probe polarization. The transformation algorithm requires both probe polarizations. If only a single polarization is available, a null signal will be assumed for the alternate polarization. The final parameter group specifies whether or not confirmation plots of the acquired data are to be generated on the graphic CRT display.

In order to transform near-field antenna data into far-field data, the transformation algorithm must be provided with a phase pattern as well as an amplitude pattern. To obtain the phase of the received signal, a phase reference is required. This does not usually pose a problem in a short near-field range. A coupler is used to sample the test signal feeding the probe, which is normally the transmitting antenna. A cable carries the signal to the receiver input where it is used as a phase reference. This cabling configuration provides a phase reference

which is independent of the probe polarization.

On an outdoor range, it is not always possible to run a cable between the signal source and the receiver. Thus, an alternate method of obtaining a phase reference is required. One technique is to station an auxiliary antenna near the receiving antenna. The orientation and/or polarization characteristics of the auxiliary antenna are arranged to provide a strong reference signal for both orientations of the probe antenna. A problem associated with this technique is that the phase reference is no longer independent of the probe orientation. Special provisions for phase compensation must be provided to eliminate the variation with probe position. In general, a different compensation must be provided for each of the test frequencies.

### Spherical Near-Field Data Transformation

The procedure for specifying the transformation of antenna data is similar to the procedure for specifying the acquisition of data. Figure 13 is a listing of the transformation test file used to generate the processed data shown in the next section. The transformation parameters are divided into a number of parameter groups as were the acquisition parameters.

The first parameter group specifies the names of the data files containing the input data. In the current version of the Model 2022, a given data file contains data for only one polarization of the probe antenna. Two data files are required to record both probe polarizations. The test frequency number is also specified. Only one test frequency undergoes transformation at a time. If the

phase reference for the acquired data was dependent on the orientation of the probe, signal correction must be performed by specification of the proper compensation parameters.

The second parameter group is the transformation control group. In this group, the operator specifies the size of the minimum sphere, the initial and final range lengths, and the pattern normalization procedure to be used. The size of the minimum sphere controls the number of spatial frequency modes considered during the pattern transformation. If the size of the minimum sphere is decreased, the number of spatial modes is also decreased. By specifying a large minimum sphere for data acquisition and a small minimum sphere for data transformation, a high degree of noise rejection can be achieved.

Also specified in this parameter group are the initial and final range lengths. Unless the operator respecifies the acquisition range length, the value specified during the preparation of the acquisition test file will be used. Note that the only restriction on the range length of the transformed data is that it be greater than the radius of the minimum sphere. Thus, the transformation algorithm can be applied to data collected in the far-field in order to generate near-field data. Alternatively, the algorithm can be used to transform data from one near-field range length to a second near-field range length.

The third and fourth parameter groups are used to specify the region of the sphere over which the data transformation will be performed. Note that the computation need not be based on a full sphere. The Model 2022 is capable of performing computation on a partial sphere of data as well. Partial sphere data sets are centered either at the north pole, the equator, or the south pole of the

\*SPHERICAL NEAR-FIELD DATA TRANSFORMATION TEST FILE NUMBER: 67

1. INPUT DATA SPECIFICATIONS
  - \*INPUT FROM SNF RASTER SCAN DATA.
  - \*SNF RASTER SCAN DATA INPUT FILE A:  
DF004
  - \*SNF RASTER SCAN DATA INPUT FILE B:  
DF005
  - \*INPUT FREQUENCY NUMBER:  
1
  - \*APC SIGNAL CORRECTION NOT PERFORMED.
2. TRANSFORMATION CONTROL SPECIFICATIONS
  - \*DATA TRANSFORMATION PERFORMED.
  - \*RADIUS OF MINIMUM SPHERE (CENTIMETERS):  
AS PREVIOUSLY SPECIFIED
  - \*RANGE LENGTH FOR INPUT DATA (CENTIMETERS):  
AS PREVIOUSLY SPECIFIED
  - \*RANGE LENGTH FOR TRANSFORMED DATA (CENTIMETERS):  
INFINITE
  - \*PATTERN PEAK NORMALIZATION PERFORMED.
  - \*RANGE LENGTH COMPENSATION PERFORMED.
3. COMPUTATION SCAN PARAMETERS
  - \*DESIRED COMPUTATION SCAN INCREMENT (DEGREES):  
ACQUISITION SCAN INCREMENT
  - \*DESIRED COMPUTATION SCAN START ANGLE (DEGREES):  
ACQUISITION SCAN START ANGLE
  - \*DESIRED COMPUTATION SCAN STOP ANGLE (DEGREES):  
ACQUISITION SCAN STOP ANGLE
4. COMPUTATION STEP PARAMETERS
  - \*DESIRED COMPUTATION STEP INCREMENT (DEGREES):  
ACQUISITION STEP INCREMENT
  - \*DESIRED COMPUTATION STEP START ANGLE (DEGREES):  
ACQUISITION STEP START ANGLE
  - \*DESIRED COMPUTATION STEP STOP ANGLE (DEGREES):  
ACQUISITION STEP STOP ANGLE
5. SNF COMPUTATION DATA OUTPUT FILE:
  - \*DATA OUTPUT FILE GENERATED.
6. SNF RASTER SCAN DATA OUTPUT FILE A:
  - \*OUTPUT POLARIZATION PARALLEL TO STEP (THETA) AXIS.
  - \*DESIRED OUTPUT SCAN INCREMENT (DEGREES):  
.250
  - \*DESIRED OUTPUT SCAN START ANGLE (DEGREES):  
COMPUTATION SCAN START ANGLE
  - \*DESIRED OUTPUT SCAN STOP ANGLE (DEGREES):  
COMPUTATION SCAN STOP ANGLE
  - \*DESIRED OUTPUT STEP INCREMENT (DEGREES):  
1.000
  - \*DESIRED OUTPUT STEP START ANGLE (DEGREES):  
90.000
  - \*DESIRED OUTPUT STEP STOP ANGLE (DEGREES):  
90.000
7. SNF RASTER SCAN DATA OUTPUT FILE B:
  - \*OUTPUT POLARIZATION PARALLEL TO STEP (THETA) AXIS.
  - \*DESIRED OUTPUT SCAN INCREMENT (DEGREES):  
COMPUTATION SCAN INCREMENT
  - \*DESIRED OUTPUT SCAN START ANGLE (DEGREES):  
22.240
  - \*DESIRED OUTPUT SCAN STOP ANGLE (DEGREES):  
23.000
  - \*DESIRED OUTPUT STEP INCREMENT (DEGREES):  
.750
  - \*DESIRED OUTPUT STEP START ANGLE (DEGREES):  
.000
  - \*DESIRED OUTPUT STEP STOP ANGLE (DEGREES):  
179.000
8. SNF RASTER SCAN DATA OUTPUT FILE C:
  - \*DATA OUTPUT FILE NOT GENERATED.
9. SNF RASTER SCAN DATA OUTPUT FILE D:
  - \*DATA OUTPUT FILE NOT GENERATED.

\*END OF TEST FILE LISTING

Figure 13. Spherical Near-Field Transformation Test File

scanning sphere. Substantial reductions in data processing time can be achieved through the use of this feature.

If the operator selects the default values for the computation scan and step parameters, the computer will choose the smallest permissible computation region which contains the acquisition region. Antenna data which is required by the transformation algorithm and has not been acquired will be assumed equal to a null signal. If the operator overrides the default parameter values and specifies a computation region which is smaller than the acquisition region, the antenna data outside the computation region will be ignored in the calculation of the transformed pattern.

The remaining parameter groups specify the generation of output data files. Up to four raster scan data files may be generated. In addition, a special computation data file may be generated. The raster scan output data files are identical in structure to the data files used for input. They may be plotted or listed in the conventional fashion. For convenience, the operator will usually extract only a portion of the transformed data for storage as raster scan data files. For example, the operator may require only the co-polarized principal plane cuts from the transformed antenna data.

Upon occasion, however, it will be necessary to extract additional information from the transformed antenna data. In this circumstance, the operator can avoid repeating the lengthy data transformation process by saving the computation data output file. This is a special data file which contains the entire transformed antenna pattern. The data in this file cannot be accessed directly. To extract information from this data file, a new transformation test file must be prepared. In the first parameter group, the name of the computation data file must be speci-

fied. In the second parameter group, the operator must specify that no data transformation is to be performed. In the last four parameter groups, the operator indicates the additional antenna data to be extracted.

To reduce the time required for data acquisition and for data transformation, the sample intervals are chosen as large as possible without exceeding the theoretical maximum interval. The transformation algorithm does not alter the sampling rate. Thus, the transformed data is sampled at the same spacing as the input data. While the coarse spacing is adequate for data acquisition and data transformation, it does not directly provide the sample density needed for good data display.

The Model 2022 overcomes this problem by providing reconstruction modules which calculate pattern points between the sampled data points. These modules are used in the generation of raster scan data output files and are automatically invoked when they are required. If the specified output increment is less than the computation increment, pattern reconstruction is performed. It should be noted that the intermediate pattern points determined by the reconstruction software are exact. No approximations are used as in certain other interpolation methods.

### Spherical Near-Field Example

As part of the development program for spherical near-field, a series of verification tests were performed. A verification antenna and adjustable mounting fixtures were designed and constructed. The antenna was then tested using both spherical near-field scanning and the Scientific-Atlanta Model 5751

Compact Range. By comparing the results of the tests, the correct operation of the spherical near-field software was established. In addition, the verification testing provided an opportunity to establish the performance level of the software. The test program was performed at the Scientific-Atlanta Gwinnett Range facility.

Figure 14 is a photograph of the antenna and positioner used for verification testing. The antenna is a 2 foot diameter parabolic reflector. Tests were performed at 13 GHz and 14 GHz. To enhance the accuracy of the measurements, optical instruments were used in conjunction with the special mounting hardware to perform range alignment.

The positioner shown in Figure 14 is the standard positioner offered with the Model 5751 Compact Range. The axis order for this positioner is roll over azimuth over elevation. For the duration of the testing, the roll and azimuth axes were used as the two active axes. The elevation axis was blocked to prevent extraneous motion. In addition to the axes listed above, a linear axis below the elevation positioner provided travel along the range axis. This motion proved useful for testing at different near-field range lengths and for checking the accuracy of the compact range.

In Figure 14, the test antenna is shown mounted in a polar configuration. Testing was also performed with the antenna mounted in an equatorial configuration. The latter configuration was obtained by the insertion of a right-angle bracket between the base of the antenna and the mounting surface of the roll positioner. In effect, the right-angle bracket converted the roll over azimuth configuration to an elevation over azimuth configuration.

The data shown on the following pages was obtained with the equatorial mounting configuration. Figure 15 summarizes the verification test from which the results have been taken. To help orient the reader, a three-dimensional plot of the far-field radiation pattern in this configuration is shown in Figure 16. In Figure 16, the azimuth (theta) axis is the scan axis and the roll (phi) axis is the step axis.

Some general comments concerning Figures 17 through 22 are in order. These figures are various amplitude comparisons made in the theta principal plane. The theta principal plane is the plane which contains the poles of the test sphere and which passes through the peak of the radiation pattern (i.e., phi equal to zero cut). In each case, the probe was vertically polarized or co-polarized to the test antenna. With the exception of Figure 21, the angular scale is  $\pm 45^\circ$  and the angle coordinates have been normalized to the peak of the radiation pattern. In Figure 21, the angular scale is  $\pm 180^\circ$  and normalization of the angle coordinates has not been performed.

Figure 17 is a comparison of the acquired near-field data and the transformed far-field data. Both patterns are sampled every  $0.75^\circ$ , which is the increment used for both data acquisition and data transformation. This figure shows the effect of the transformation process.

Figure 18 is a comparison of the reconstructed far-field pattern to the coarsely sampled far-field pattern. The reconstructed pattern has a sample increment which is  $0.25^\circ$ , compared to the original increment of  $0.75^\circ$ . As can be seen, the reconstructed pattern produces a much better representation of the antenna.

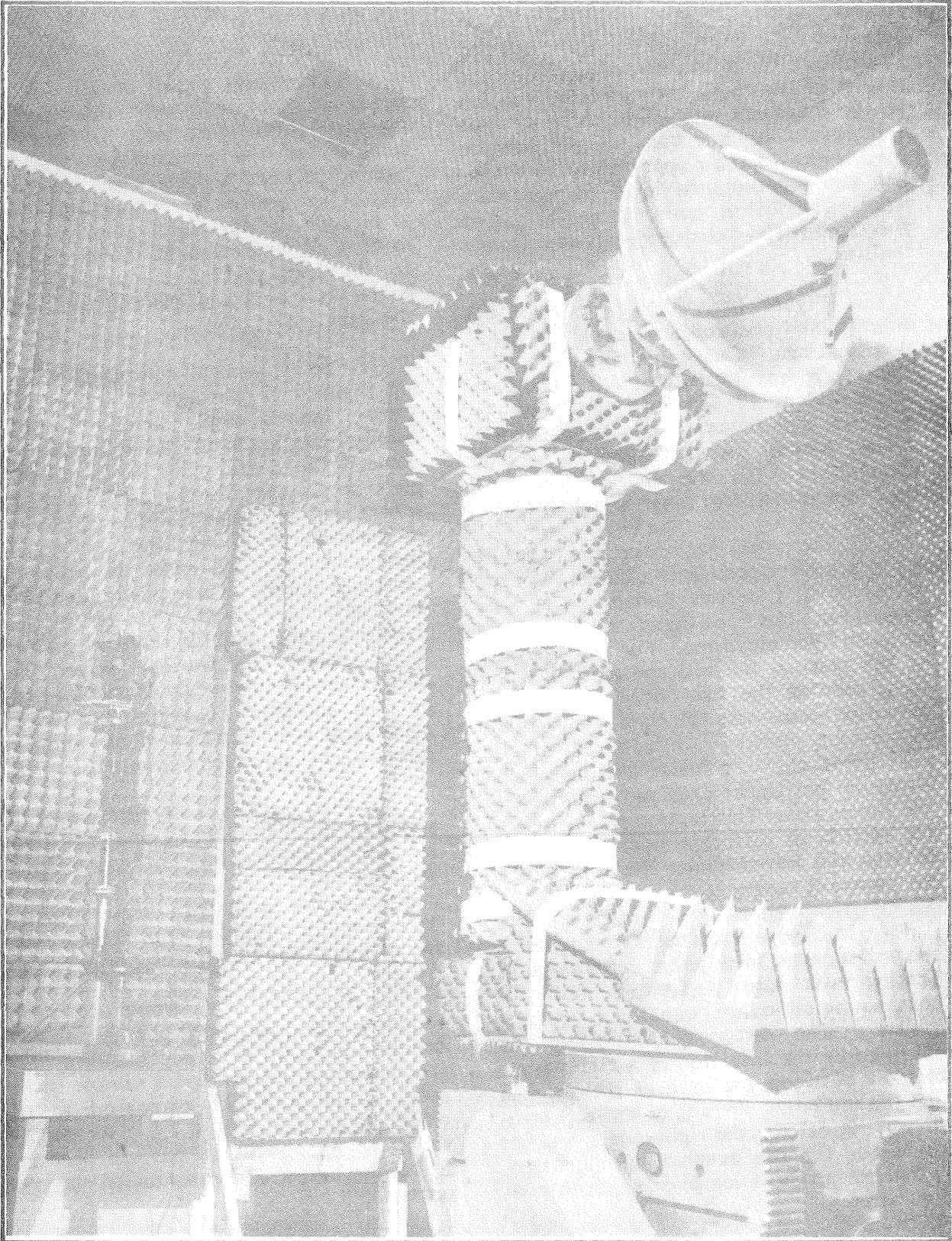
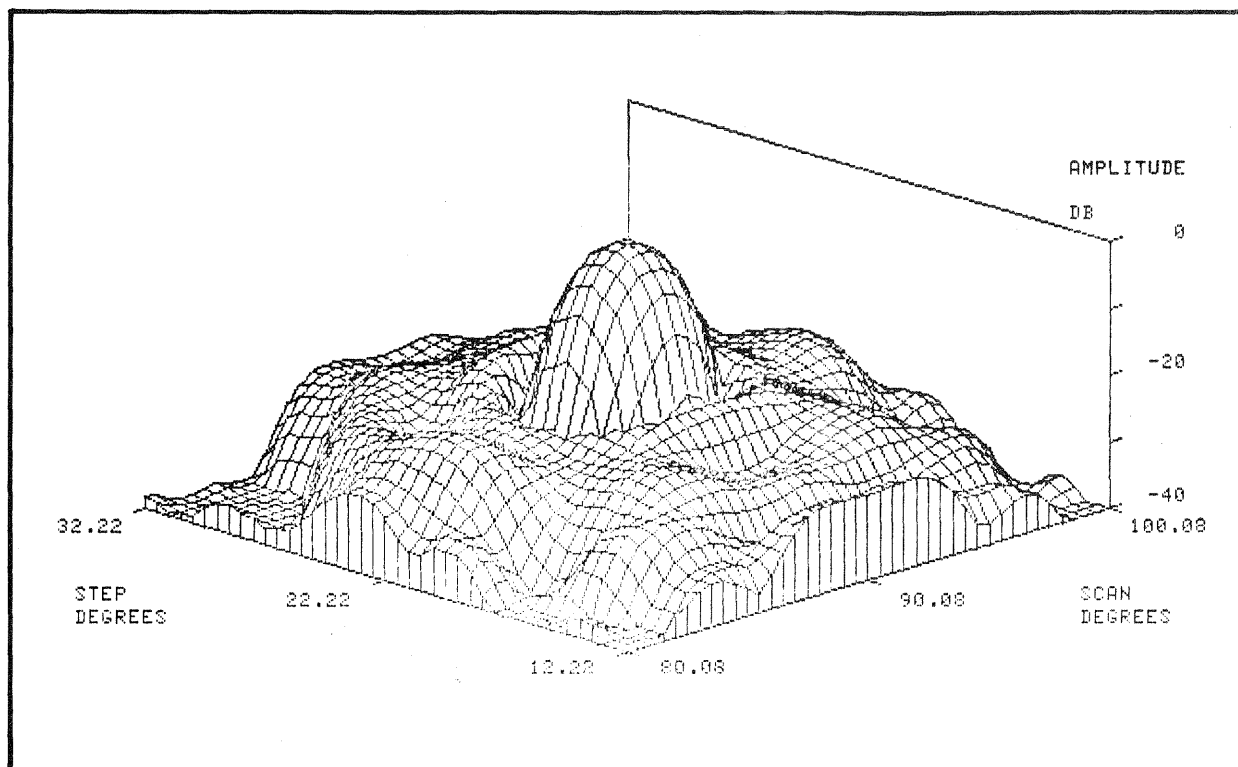


Figure 14. Antenna Used in Verification Tests

Antenna	24 in. (61 cm) Diameter Parabolic Reflector
Positioner	Roll over Azimuth
Mounting Configuration	Equatorial (Right angle bracket attaches antenna to roll axis)
Beam Maximum Position	22.24° Roll, 90.09° Azimuth
Radius of Minimum Sphere	34 in. (86 cm)
Test Frequency	13 GHz
D/λ Ratio	75
Near-Field Range Length	117.8 in (299.2 cm)
Far-Field Range Length	Infinity

**Figure 15. Equatorial Verification Test Parameters**



**Figure 16. Far-Field Radiation Characteristics of Verification Antenna**

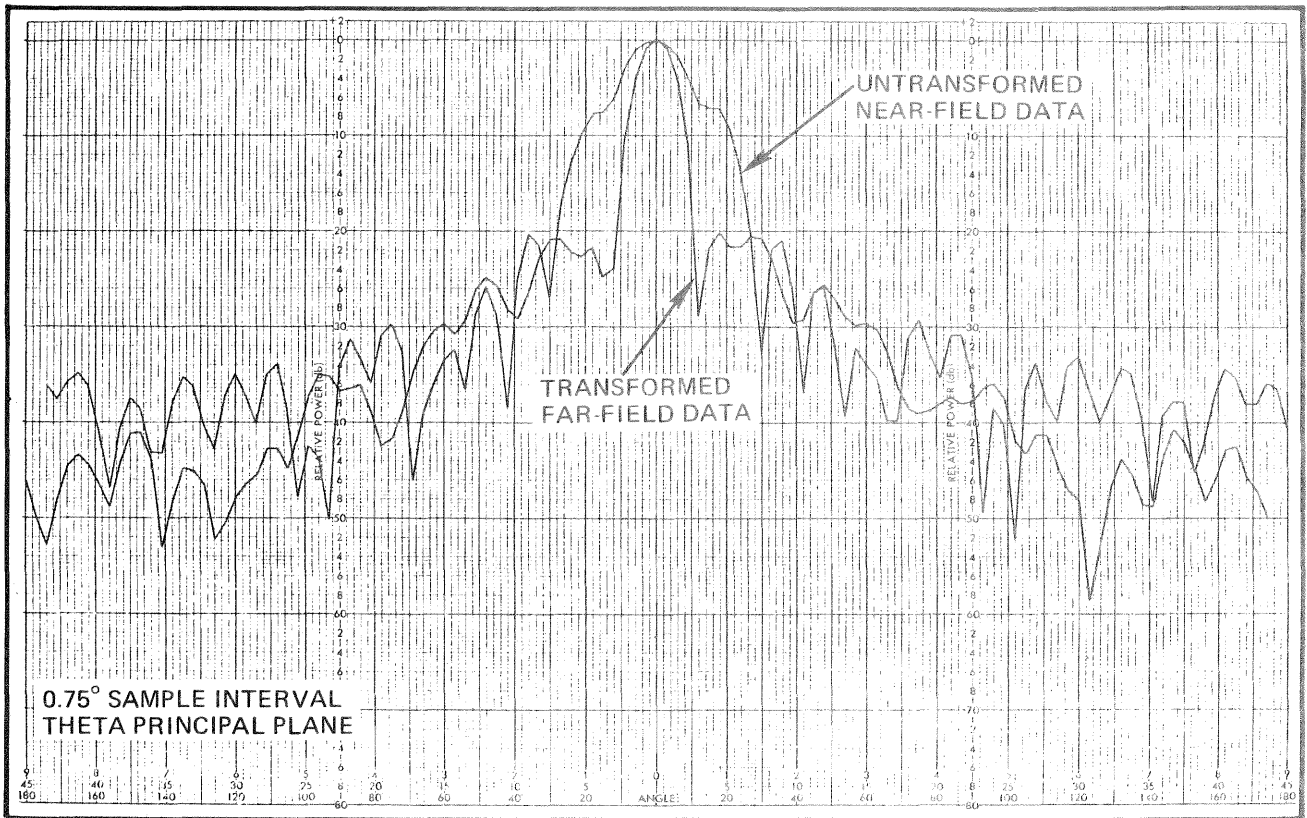


Figure 17. Far-Field Data vs. Near-Field Data

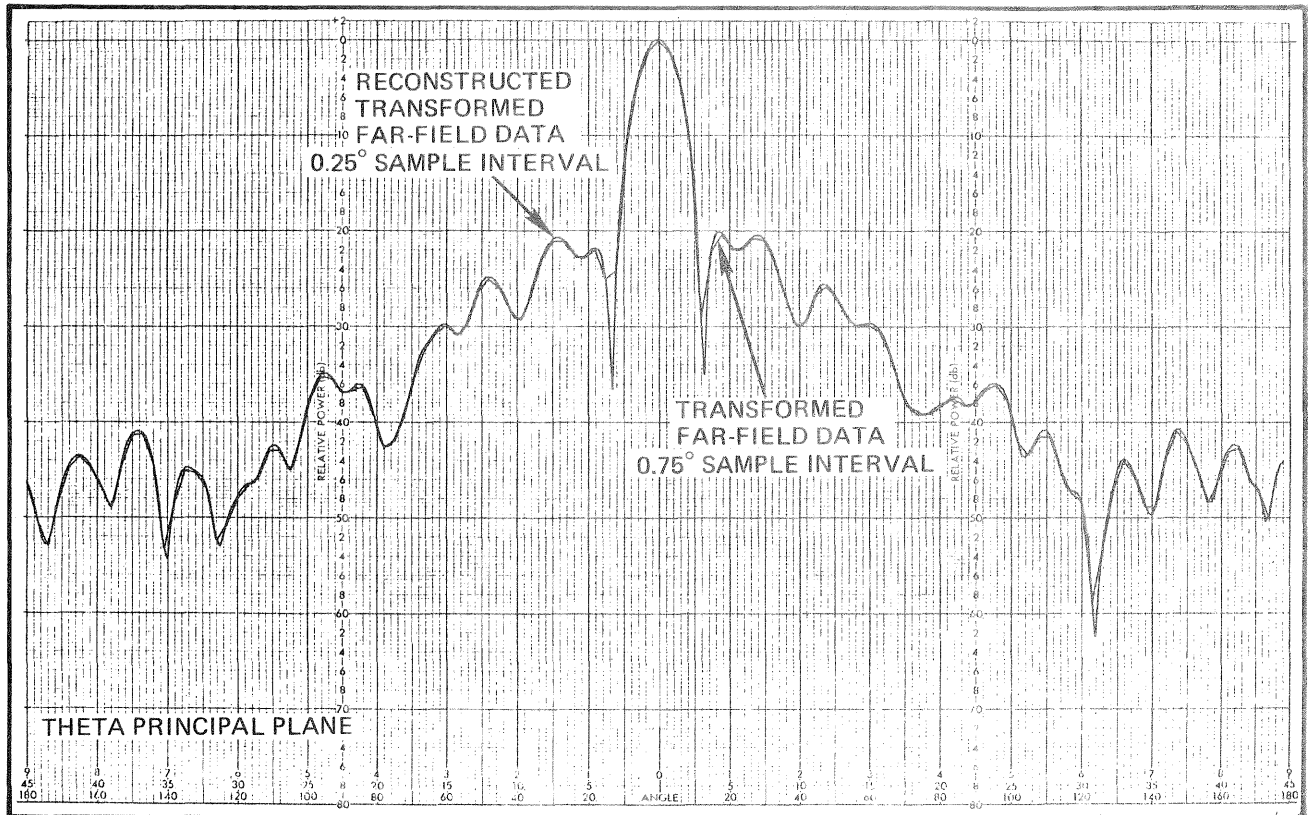


Figure 18. Reconstruction of Far-Field Pattern

Before comparing the spherical near-field test results to the compact range test results, the accuracy of the compact range was established. Inaccuracies in the compact range were predominantly caused by stray signal reflections. To characterize these inaccuracies, several pattern measurements were made at various positions along the range axis. Thus, the stray signal radiation was dephased with respect to the planar wavefront from the compact range reflector. The various positions produced discrepant patterns which indicate the performance level of the range. This type of performance characterization is dependent on the test antenna as well as on the inherent accuracy of the compact range, since the antenna possesses its own directional properties. Figure 19 illustrates the results of this measurement procedure.

Figure 20 is a comparison of the far-field pattern obtained with spherical scanning and one of the patterns obtained with the compact range. Figure 21 presents the same comparison, but over the entire  $360^\circ$  cut. The spherical near-field results and the compact range results match to within the reproducibility of the experiment and the accuracy of the compact range.

Finally, Figure 22 presents the outcome of a partial sphere transformation. The transformation shown is for a  $60^\circ$  by  $60^\circ$  patch centered at the equator of the test sphere. The same input data which was used for the full sphere transformation provided input data for the partial sphere transformation. As can be seen, the partial sphere result is essentially unchanged from the full sphere result over most of the pattern.

Spherical scanning on a partial sphere provides a substantial time savings in both data acquisition and data transformation. The time required to collect data for full sphere used in the preceding test was greater than 8 hours. The time required to collect data over the  $60^\circ$  by  $60^\circ$  partial sphere would have been less than 1 hour. The time required to generate the transformed antenna patterns, including the time required for input data processing and output data processing, was 5-1/2 hours for the full sphere, as compared to 1 hour for the partial sphere. Thus, the total test time is reduced from over 13-1/2 hours to under 2 hours via the use of partial spheres.

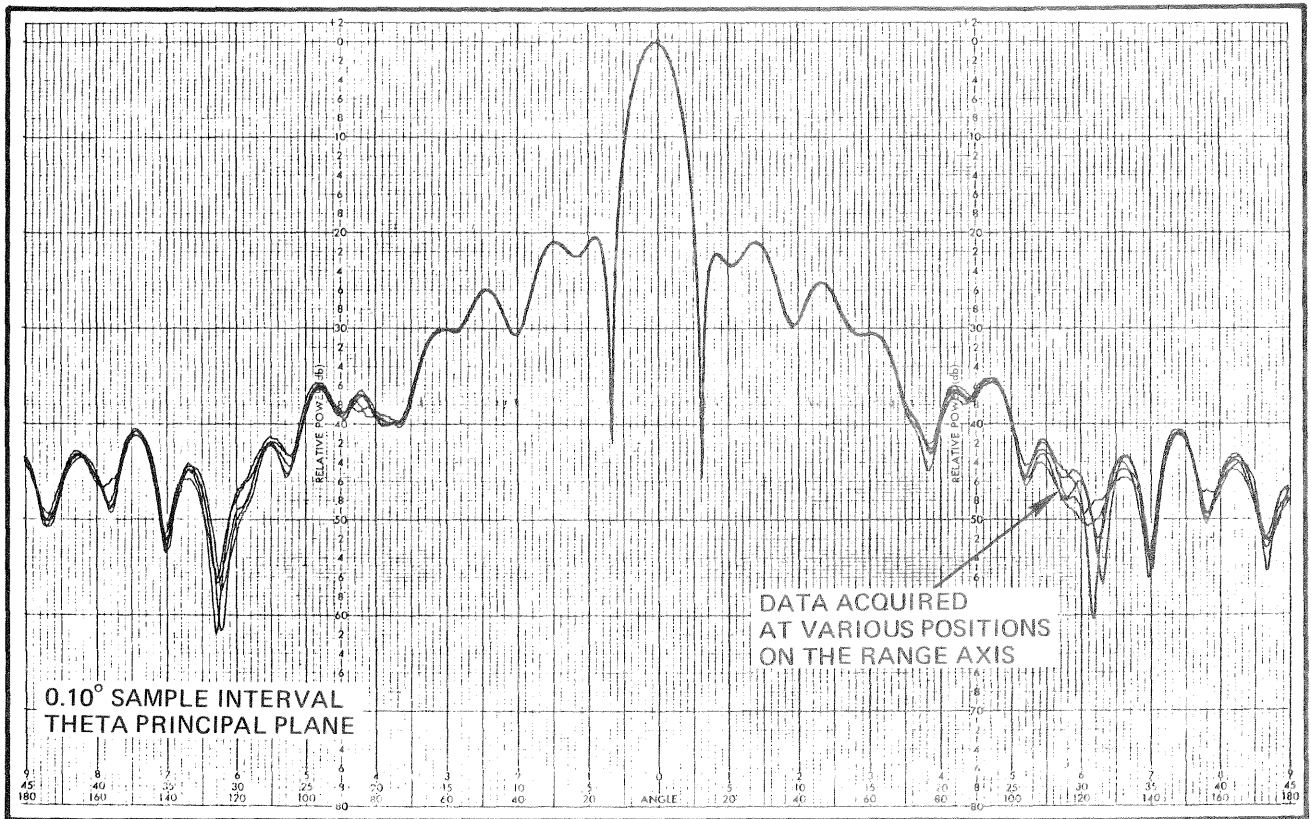


Figure 19. Determination of Compact Range Accuracy

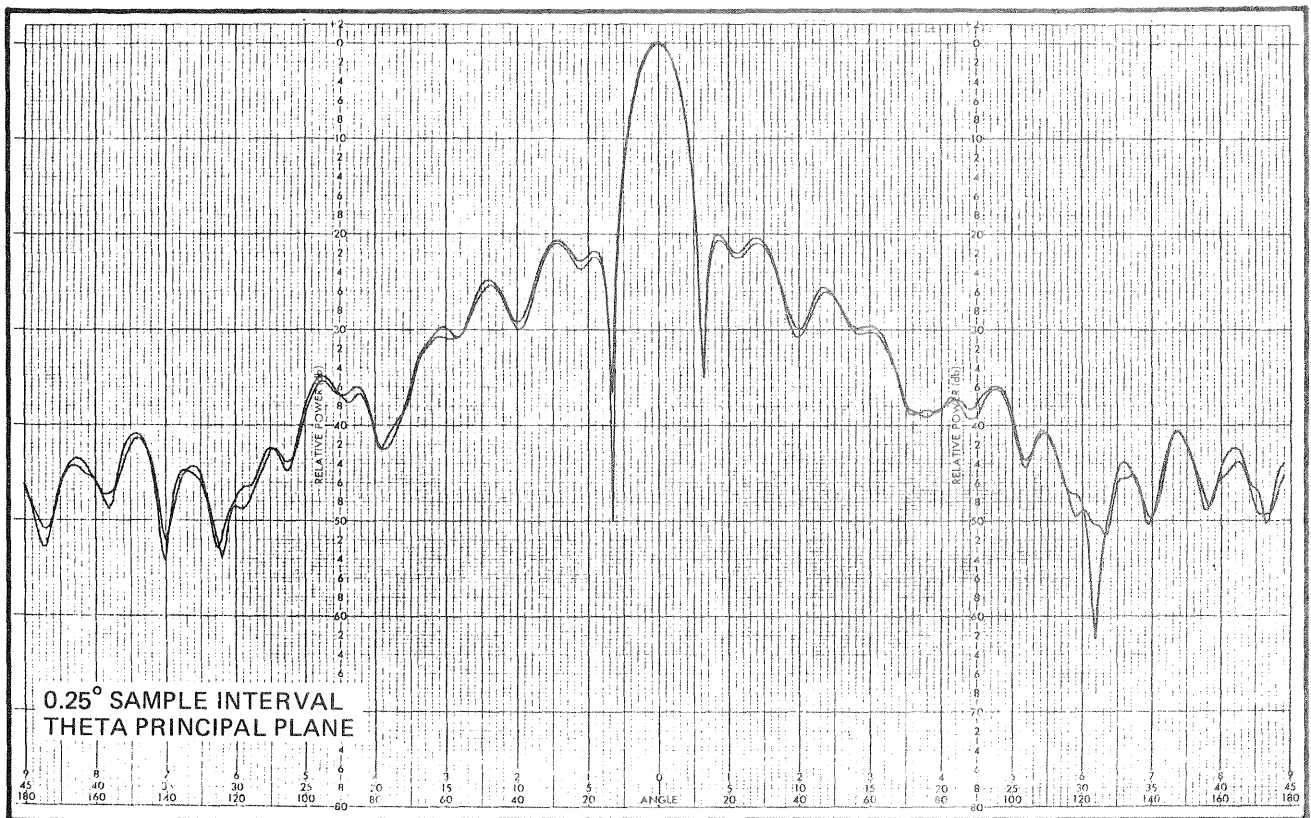


Figure 20. Transformed Data vs. Compact Range Data

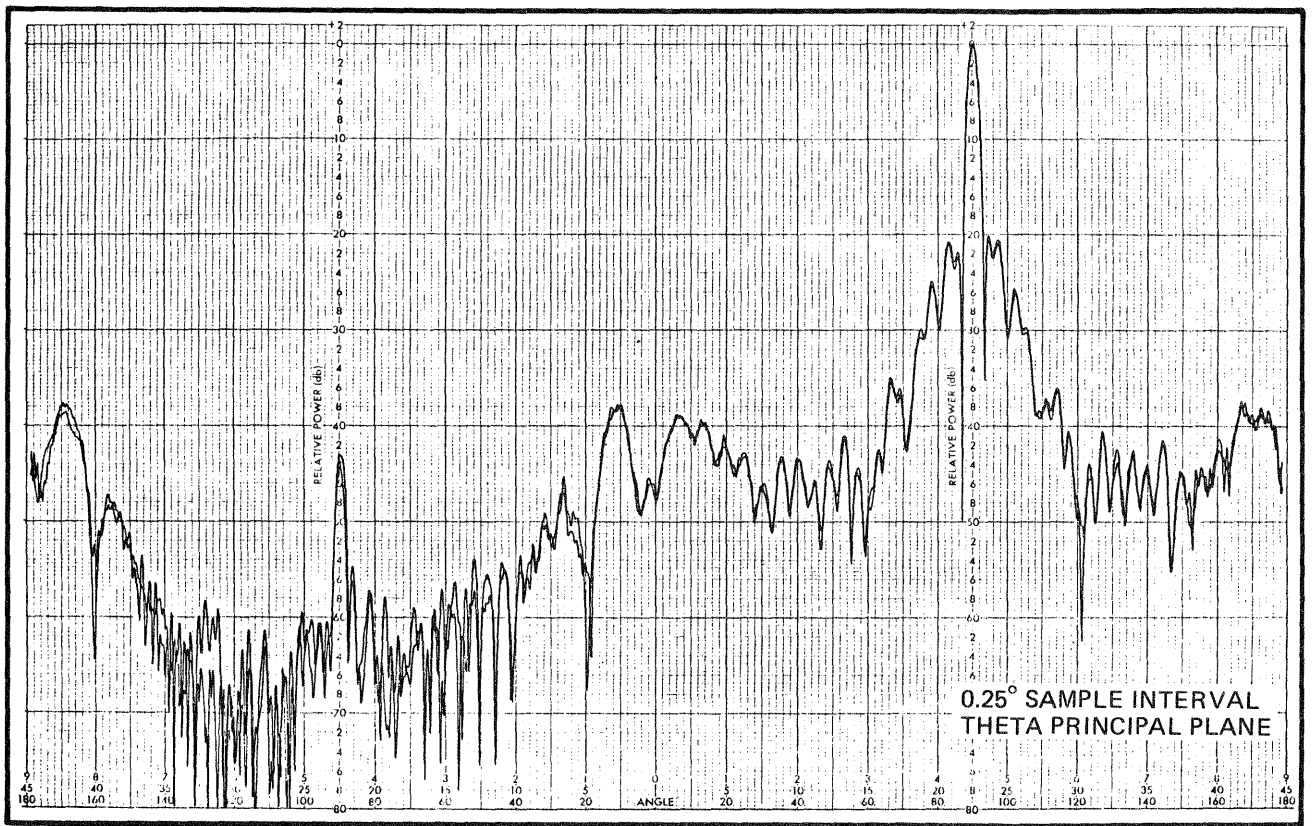


Figure 21. Transformed Data vs. Compact Range Data

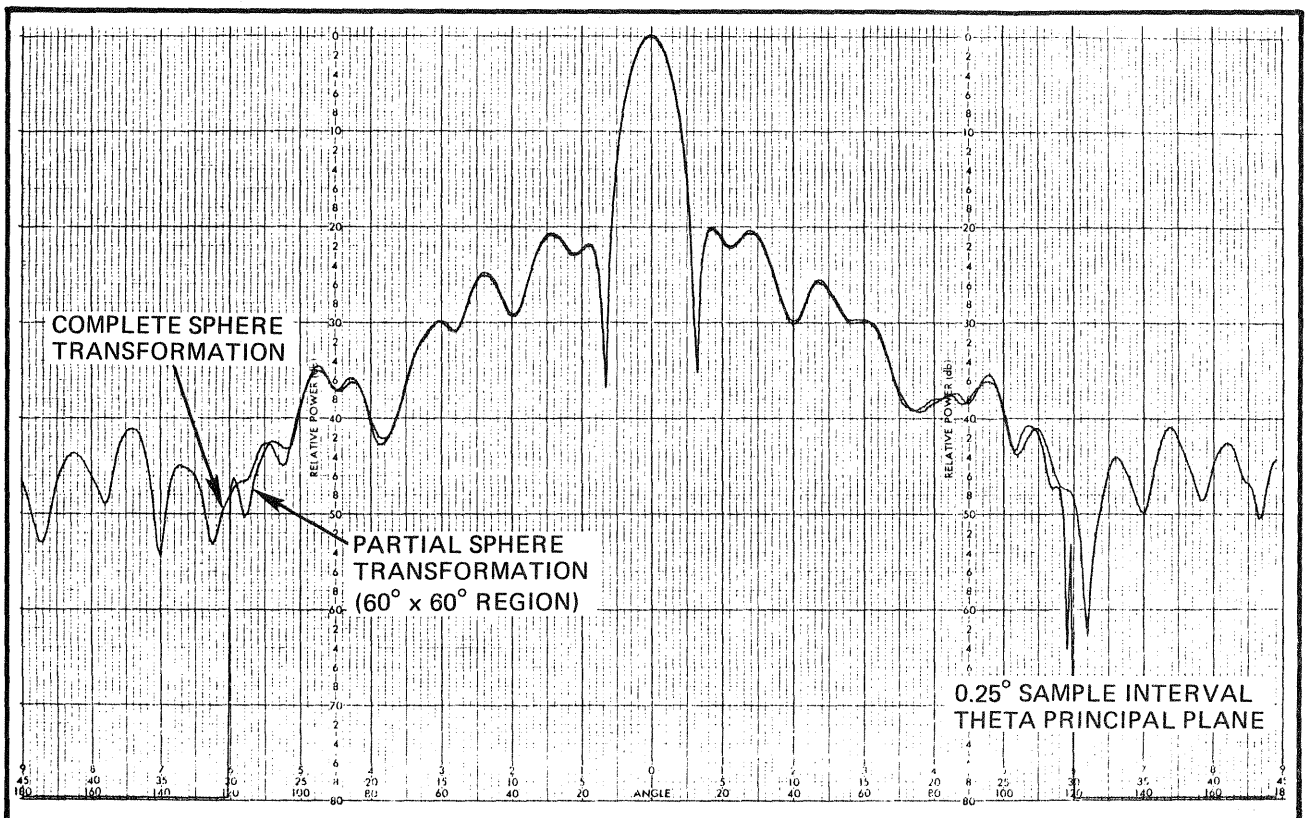


Figure 22. Transformation on Partial Sphere vs. Transformation on Complete Sphere

## Conclusion

Spherical near-field scanning offers several advantages over conventional antenna test methods. In certain test situations, spherical near-field is the best test method. The relative advantages and disadvantages of spherical near-field have been described. Key concepts required to understand and use the spherical near-field technique have been defined.

The Scientific-Atlanta Model 2022, which is an implementation of the spherical near-field test method, has been described. The antenna test engineer

controls near-field data acquisition and near-field data transformation through a conversational interface. The near-field software implemented by Scientific-Atlanta provides an easy to use, flexible, and powerful antenna test capability.

Antenna data obtained via the spherical near-field capability of the Model 2022 has been presented. The near-field measurements have been verified using compact range antenna measurements. Spherical near-field has been shown to be an important antenna test method.

## References

1. Scientific-Atlanta, Inc., "The Compact Range", Microwave Journal, October 1974, p 30.
2. Johnson, R. C., Ecker, H. A., and Moore, R. A., "Compact Range Techniques", IEEE Transactions, APS-17,568, 1969.
3. Joy, Edward B. and Paris, Demetrius T., "Spatial Sampling and Filtering in Near-Field Measurements", IEEE Transactions, APS-20,253, 1972.
4. Newell, Allen C. and Crawford, Myron L., "Planar Near-Field Measurements on High Performance Array Antennas", National Bureau of Standards, Boulder, Colorado, 1974, Report Number NBSIR 74-380.
5. Merscreau, Russell M., "The Processing of Hexagonally Sampled Two Dimensional Signals", Proceedings of the IEEE, June 1979, Vol. 67, No. 6, Paper Number 0018-9219/79/0600-9030.
6. Wacker, Paul F., "Plane-Radial Scanning Techniques with Probe Correction; Natural Orthogonalities With Respect to Summation on Planar Measurement Lattices", IEEE Antennas and Propagation Society International Symposium 1979, Paper Number CH1456-3/79/000-0561.
7. Wacker, Paul F., "Non-Planar Near-Field Measurements: Spherical Scanning", National Bureau of Standards, Boulder, Colorado, 1975, Report Number NBSIR 75-809.
8. Jensen, F., "On the Probe Compensation for Near-Field Measurements on a Sphere", Arch. Elektron & Ubertragungstech, 1975, Vol. 29, pp 305-308.
9. Larsen, F. H., "Improved Algorithm for Probe-Corrected Spherical Near-Field/Far-Field Transformation", Electronics Letters, September 1979, Vol. 15, No. 19, pp 588-590.
10. Hansen, J. E., "Spherical Near-Field Testing of Spacecraft Antennas", ESA Journal, 1980, Vol. 4, p 89.